RSC Advances

ROYAL SOCIETY OF CHEMISTRY

www.rsc.org/advances

RSC Advances

ARTICLE

Biologizing titanium alloy implant material with morphogenetically active polyphosphate

Received 00th January 20xx,
Accepted 00th January 20xx

DOI: 10.1039/x0xx00000x

www.rsc.org/

Werner E.G. Müller[a,§], Emad Tolba[a], Heinz C. Schröder[a], Shunfeng Wang[a], Gunnar Glasser[b], Bärbel Diehl-Seifert[c] and Xiaohong Wang[a,§]

As a further step towards a new generation of bone implant materials, we developed a procedure for biological functionalization of titanium alloy surfaces with inorganic calcium polyphosphate (Ca-polyP). This polymer has been demonstrated to exhibit morphogenetic activity. The coating of titanium oxidized Ti-6Al-4V scaffolds with biologically active amorphous Ca-polyP microparticles is formed by Ca^{2+} ion bridges to the silane coupling agent APTMS. This surface is durable and stable as an almost homogeneous Ca-polyP layer onto the metal. The homogenously coated Ca-polyP titanium scaffold was found to be biologically active and supported the growth and functional activity of bone cell-related SaOS-2 cells despite of the reduced surface roughness, while the non-modified titanium surfaces are biologically inert. Quantitative qRT-PCR experiments revealed that the Ca-polyP coated titanium alloy markedly increased the steady-state levels of transcripts of the two marker enzymes involved in initiation of bone mineral deposition, the carbonic anhydrase IX and the alkaline phosphatase. The innovative coating of titanium alloy with Ca-polyP offers a promising technique for the fabrication of morphogenetically active bone implants with advantageous mechanical and regeneration-inducing properties.

Introduction

Skeletal defects, resulting from traumatic, infectious, congenital or neoplastic processes, have been tried to be restored by a series of approaches, starting from the Greek/Roman time (reviewed in: ref.[1]). Orthopedic implants are inserted when non-surgical methods of treatment failed. In order to reconstitute bone defects with the aim to stabilize the failure, traditional inorganic materials, e.g. gold, silver, lead and aluminum have initially been used, which turned out to be too weak, or iron, steel, copper etc have been applied, which showed adverse responses. In parallel alloplastic materials, both of biological (ivory, corals) and non-biological origin (metal, ceramics, and plastics) have been tried. However, it has always been the imagination to fabricate an implant that has the property to allow reconstitution of the bone defect by regeneration followed by functional recovery. Surely *autografts*, using bone grafts from the same individual will remain the "gold standard";[2] in addition, successful approaches and processes have been developed and outlined using *allografts*, consisting of autogenous bone material from a different individual as well as *xenografts*, taken from species other than human e.g. corals, to substitute and repair bone defects.[3]

In line with other major prerequisites for being a suitable regeneratively active scaffold, to be biodegradable and likewise osteoinductive,[4] as well as to allow the adjustment of the mechanical properties of the implant material towards the bordering bone tissue, we developed a morphogenetically active inorganic scaffold material, which is based on amorphous polyphosphate (polyP).[5,6] Following the basic principles of morphogenesis, polyP is not only related but also directly involved in the development of normal organic patterns and tissues. Previously it has been described that polyP regulates cell-specific differentiation processes, like the formation of mineral depositions onto bone-forming osteoblasts with the model cell line SaOS-2 cells and the induction of the alkaline phosphatase (ALP) and shifts the OPG (osteoprotegerin):RANKL (receptor activator of nuclear factor κB ligand) ratio towards anabolic, osteoblast pathway and by that inhibits the function of osteoclasts, using the model cell line RAW 264.7 (reviewed in: ref.[6]). In addition, polyP induces the genes encoding for the bone morphogenetic protein-2 (BMP-2) and the scaffold structural filamentous system, the collagens.[7] Recently, amorphous polyP-based nanoparticles as well as microparticles[8,9] could be prepared that act not only in an anabolic way on the osteoblast system, but also provide metabolic fuel for their target cells, like the osteoblasts, and cause an elevation of the intracellular level of ATP as well as an increase in the number of mitochondria.[10] First animal studies with amorphous polyP particles indicate that also *in vivo* this inorganic polymer causes a structured re-organization of damaged bone tissue by accelerating a controlled regeneration of bone defects (Müller et al. submitted).

[a] *ERC Advanced Investigator Grant Research Group at the Institute for Physiological Chemistry, University Medical Center of the Johannes Gutenberg University, Duesbergweg 6, D-55128 Mainz, GERMANY. E-mails: wmueller@uni-mainz.de (W.E.G.M.); wang013@uni-mainz.de (X.H.W.)*
[b] *Max Planck Institute for Polymer Research, Ackermannweg 10, 55128 Mainz, GERMANY.*
[c] *NanotecMARIN GmbH, Duesbergweg 6, D-55128 Mainz, GERMANY.*

Since on the one hand, polyP is a versatile biopolymer that is morphogenetically active (see above) and can be used for the fabrication of implants by computer-based bioprinting processes[11,12] and on the other hand, titanium is likewise a basic material for the production of implants, by application of computer-based metal laser sintering technologies,[13] it was attractive to solve the problem of coating of titanium oxidized Ti-6Al-4V scaffolds with polyP. This alloy allows the attachment and functional differentiation of cells.[11] This task was solved by coupling of polyP to Ti–6Al–4V via a silane coupling agent, after etching/functionalization of the alloy.[14] The metal surface – after coating with polyP – turned to a biologically active platform for SaOS-2 cells that have bone cell-related properties.[15] The titanium alloy presents a suitable matrix for bone-like SaOS-2 cells to grow onto and – even more – to induce them, in contrast to the untreated titanium scaffolds to express key enzymes, the carbonic anhydrase IX (CA IX) and the alkaline phosphatase (ALP) in the initiation of enzyme-induced bone mineral deposition. Based on the data gathered, the herein described coated titanium scaffolds appear to be promising material for the fabrication of high-precision implants with innovative regeneration-eliciting characteristics.

Material and Methods

Materials

Sodium polyphosphate (Na-polyP) with an average chain length of ≈40 phosphate units was obtained from Chemische Fabrik Budenheim (Budenheim; Germany).

Ti-Ca-polyP discs

Titanium alloy (Ti–6Al–4V) disks (15 mm in diameter and 2 mm in thickness),[13] were obtained from Nobel Biocare (Göteborg; Sweden). Prior to use they were polished with emery paper (silicon carbide; Matador [Hoppenstedt, Darmstadt; Germany]) followed by ultrasonic cleaning in distilled water, and subsequently washing in acetone (10 min) and in 40% ethyl alcohol solution (15 min), and finally rinsing in distilled water for 20 min. The samples were dried at 50°C for 24 h. Then titanium alloy discs were incubated in 20 mL of 5 M HCl at room temperature for 6 h.[16] After gentle washing in distilled water the discs were dried at room temperature and the treated disc samples were overlayed with Ca-polyP nanoparticle suspension in the presence of the silane coupling agent (3-aminopropyl)trimethoxysilane [APTMS] (Sigma-Aldrich, Taufkirchen; Germany; # 281778).[17,18] Ca-polyP microparticles were fabricated as described.[8] In brief, the Ca-polyP suspensions were prepared by mixing of 0.5 g of Na-polyP with ATPMS solution (1 wt %) in 100 ml water; then 0.1 g Ca^{2+}-chloride dihydrate ($CaCl_2 \bullet 2H_2O$) was added. The titanium disks were incubated in the above suspension for 3 h at a 90°C; under those conditions a colloidal suspension was initially formed. The pH of the environment was adjusted to 8.0 to allow binding of polyP to the silane-etched titanium discs via Ca^{2+} ionic bonds/bridging. The samples remained in this suspension for 1 d. The influence of two different ATMPS concentrations (1 mg/assay and 2 mg/assay, respectively) on the morphology of the coat formed onto the titanium surface was studied. Finally, the specimens, titanium-Ca-polyP (Ti-Ca-polyP)discs, were removed and dried at 100° C (Fig. 1).

For the experiments, shown here, we were using either untreated titanium alloy discs “untreated titanium discs”, or those discs coated with polyP “Ti-Ca-polyP discs”.

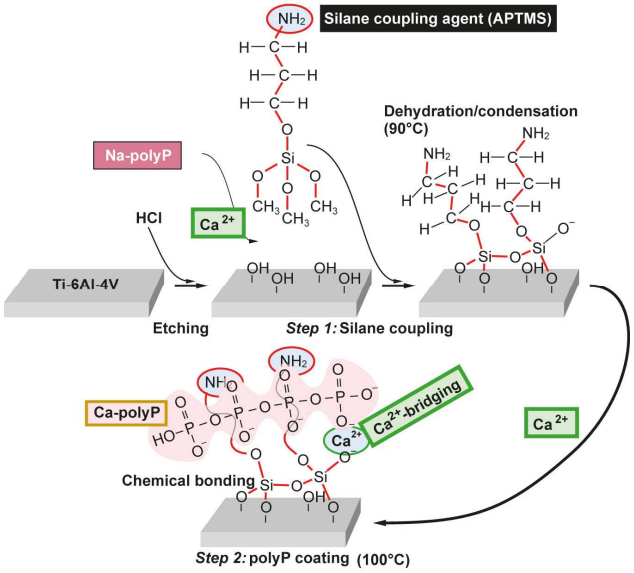

Fig. 1 Binding of polyP to titanium discs using the silane coupling agent APTMS (scheme). The titanium alloy Ti–6Al–4V is etched with HCl and the hydroxyl groups, exposed onto the titanium discs, are cross-linked with the silane coupling agent APTMS that forms Ca^{2+}-bridges to polyP. After dehydration/polycondensation the coupling agent still contains a free, reactive amine group that might be used for further coupling to active components, e.g. *via* 1-ethyl-3-(3-dimethylaminopropyl)carbodiimide. During this process the metal surface is covalently linked with the silane that in turn allows binding of polyP via Ca^{2+} ionic bridges.

Routinely, and if not mentioned otherwise, discs prepared with the higher proportion of APTMS during coating with Ca-polyP were used for the studies.

Durability of the Ca-polyP coat

The stability and the durability of the Ca-polyP coat around the titanium discs were quantified by determination of the Ca^{2+} release from the discs. The control discs, as well as the Ti-Ca-polyP discs were submersed in simulated body fluid (SBF), as described[19] but omitting Ca^{2+} as component; the pH was adjusted to 8.0. The assay volume was 1 ml and incubation was performed at 37°C. The Ca^{2+} concentration was determined by applying the complexometric titration method;[20] the reagent Eriochrome Black T was used (Sigma-Aldrich; # 858390). The surface thickness of the polyP coat on one plane of the discs was determined microscopically to be ≈ 5 µm. In turn, the total amount of Ca-polyP (density of ≈ 3 g/ml) on one plane of the discs revealed a value of ≈ 2.4 mg.

Where indicated, 5 µg of alkaline phosphatase (ALP) from bovine intestinal mucosa (Sigma; # P0114; ≥6,500 DEA units/mg protein) was added to the reaction mixture.

Microscopic analysis

The light microscopic inspection of the discs was performed with a VHX-600 Digital Microscope from KEYENCE (Neu-Isenburg; Germany), equipped either with a VH-Z25 zoom lens (25× to 175× magnification) or a VH-Z-100 long-distance high-performance zoom lens (up to 1000× magnification). The surface roughness was measured by using the KEYENCE VK-analyser software. For the scanning electron microscopic (SEM) analyses a HITACHI SU 8000 electron microscope (Hitachi High-Technologies Europe GmbH, Krefeld, Germany) was employed.

For scanning electron microscopy (SEM), an SU 8000 instrument (Hitachi High-Technologies Europe, Krefeld, Germany) was employed at low voltage (1 kV) as described.[5]

Energy dispersive X-ray spectroscopy

Energy dispersive X-ray (EDX) spectroscopy was performed with an EDAX Genesis EDX System attached to a scanning electron microscope (Nova 600 Nanolab; FEI, Eindhoven, the Netherlands) operating at 10 kV with a collection time of 30–45 s. Areas of approximately 5 μm^2 were analyzed.

EDX Hypermapping was performed with the Hitachi SU 8000 microscope[21] coupled with a Bruker XFlash 5010 detector. This combination of devices was applied at 10 kV, in order to acquire an elemental map of the deposits on the surfaces. The HyperMap database was used for interpretation, as described.[22]

Cultivation of SaOS-2 cells

Bone cell like SaOS-2 cells (human osteogenic sarcoma cells)[15] were cultured in McCoy's medium (Biochrom-Seromed, Berlin, Germany; consisting of 1 mM $CaCl_2$ and 4.5 mM NaH_2PO_4), supplemented with 2 mM L-glutamine, 10% heat-inactivated fetal calf serum (FCS), and 100 units/ml penicillin and 100 µg/ml streptomycin.[21] The cells were incubated in 25-cm^2 flasks or in 6-well plates (surface area 9.46 cm^2; Orange Scientifique, Brainel'Alleud, Belgium) in a humidified incubator at 37°C. The cultures were started with 3×10^4 cells/well in a total volume of 3 ml. After an initial incubation period of 3 d, the cultures were continued to be incubated for a total of 5 days in the absence or presence of the mineralization activation cocktail (MAC), comprising 5 mM β-glycerophosphate, 50 mM ascorbic acid and 10 nM dexamethasone to induce biomineralization.[23] For the studies with the discs, 24-well plates (Corning; Lowell, MA; diameter of each well 15.6 mm) were used into which the 15 mm large discs were inserted. The assays were performed with a total volume of 2 ml of cells/medium/FCS.

Cell proliferation/cell viability assays

Cell proliferation/growth was determined by the colorimetric method, based on the tetrazolium salt XTT (Cell Proliferation Kit II; Roche, Mannheim; Germany), following the recommendations of the supplier and as described.[24] The absorbance was determined at 650 nm and subtracted by the background values (500 nm). Routinely the viable cells were determined after 72 h.

In one series of experiments the cells on the discs, after an incubation period of 72 h, were fixed with 4% paraformaldehyde solution and then dehydrated through a series of graded ethanol solutions.[25] The specimens were then inspected by SEM.

Reverse transcription-quantitative real-time PCR analyses

The quantitative real-time RT [reverse transcription]-polymerase chain reaction (qRT-PCR) technique was applied to determine the effect of the discs on the expression levels of the following genes in SaOS-2 cells. The technique has been given previously.[21,26,27] In brief, RNA was extracted from the cells and the PCR reaction was performed using the following primer pairs: carbonic anhydrase IX (CA IX; NM_001216 human; product length of 129 bp) with the forward primer CAIX-F: 5'-ACATATCTGCACTCCTGCCCTC-3' [nt_{977} to nt_{998}] and the reverse primer CAIX-R: 5'-GCTTAGCACTCAGCATCACTGTC-3' [nt_{1105} to nt_{1083}], and the alkaline phosphatase (ALP; NM_000478.4; 278 bp) with the ALP-F: 5'-TGCAGTACGAGCTGAACAGGAACA-3' [nt_{1141} to nt_{1164}] and ALP-R: 5'-TCCACCAAATGTGAAGACGTGGGA-3' [nt_{1418} to nt_{1395}]. The glyceraldehyde 3-phosphate dehydrogenase (GAPDH) was used as a reference (NM_002046.5; product length of 217 bp) with the primer pair GAPDH-F: 5'-CCGTCTAGAAAAACCTGCC-3' [nt_{929} to nt_{947}] and GAPDH-R: 5'-GCCAAATTCGTTGTCATACC-3' [nt_{1145} to nt_{1126}]. The PCR reactions were performed in an iCycler (Bio-Rad, Hercules, CA; USA), applying the respective iCycler software. After determinations of the C_t values the expression of the respective transcripts was calculated.[28]

Statistical analysis

After determination that the values follow a standard normal Gaussian distribution, the results were statistically evaluated using paired Student's *t*-test.[29]

Results

Titanium-Ca-polyP (Ti-Ca-polyP) discs

Titanium alloy (Ti–6Al–4V) disks were etched to allow cross-linking with the silane coupling agent APTMS (Fig. 1). In the second step the discs were covered with polyP via Ca^{2+} ionic bridges. Finally the specimens, the Ti-Ca-polyP discs, were dried at 100°C. We used – on purpose – the silane coupling agent APTMS to provide a further functional group, an amine group, to couple also bioactive peptides to the polyP-coated metal surface. The functionalization of the titanium discs has also been performed with 3-(trimethoxysilyl)propyl methacrylate[30] successfully allowing a polyP-titanium coating only (not shown here).

Fig. 2 Comparison between an untreated, dark gray titanium alloy disc (left) and a Ti-Ca-polyP disc (right); light microscopic image.

A comparison between the titanium alloy discs and the Ti-Ca-polyP discs (light microscopic images) is shown in Fig. 2. In contrast to the dark gray surface color of the titanium alloy discs, the Ti-Ca-polyP discs have a shiny silver-white appearance. After the coating of the surfaces of the discs with polyP they lose their high roughness. While the untreated discs have an average roughness of ≈ 5.5 µm with a maximum of 7.02 µm (Fig. 3A, C, E) the polyP coated discs expose a surface roughness of 0.78 µm in maximum (Fig. 3B, D, F).

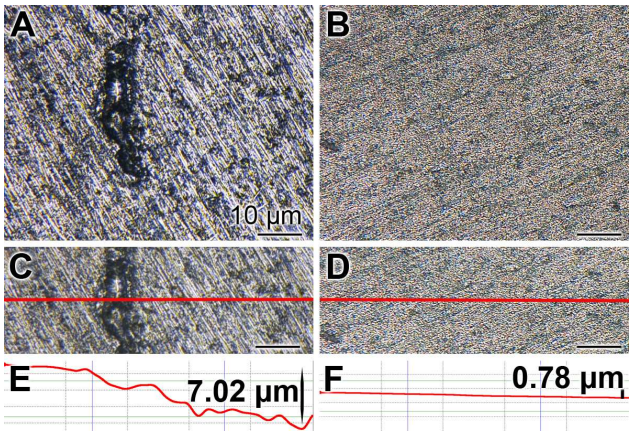

Fig. 3 Surface roughness of the titanium alloy discs (**A**, **C**, **E**) in comparison with the Ti-Ca-polyP discs (**B**, **D**, **F**). The surfaces of the discs were visualized by light microscopy and analyzed for roughness using the VK-analyser software. The tracks of the line-scans (C, D) are shown as red lines. The height profiles of representative regions are shown in E, F; the numbers indicate the maximal dimensions for the deviations within a normal vector straight line.

Element-specific analyse of the surfaces of the titanium discs was performed by EDX spectroscopy (Fig. 4). The surface of the non-treated discs showed the dominant K_α peak for titanium at 4.5 keV and the lower K_β peak at 4.9 keV (Fig. 4A). The morphology of the surface is marked rough (Fig. 4B). If the titanium discs, after etching and reacting with the lower concentration of APTMS (1 mg/assay), are examined after an incubation in the coating solution with polyP and $CaCl_2$, Ca-polyP microparticles[9] can be resolved by SEM (Fig. 4D). The size of the particles varies between 0.8 and 3 µm.

After drying the discs at 100°C the EDX determinations were performed. A representative spectrum (Fig. 4C) shows the now dominant K_α peak for phosphorus at 2.01 keV. In addition, the calcium peak (3.69 keV) is detectable. The titanium peak (4.5 keV) is recordable as well. If the disc samples coated with polyP after addition of the higher amount of APTMS (2 mg/assay) are inspected by SEM an almost homogeneous polyP surface can be visualized by SEM (Fig. 4F). This observation is supported by the EDX measurements that revealed a (almost) complete disappearance of the titanium peak (Fig. 4E), while the phosphorus and calcium peaks become dominant.

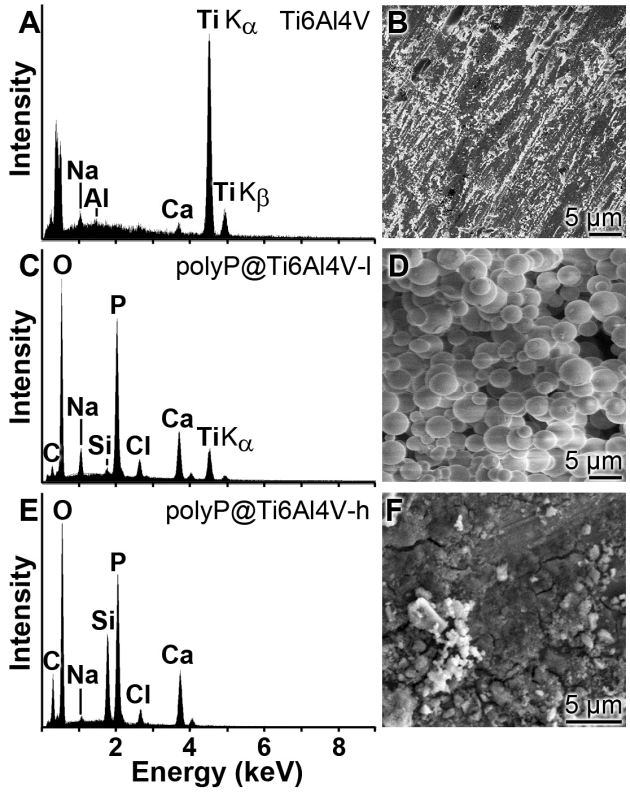

Fig. 4 Analysis of the element composition of the titanium and Ti-Ca-polyP discs by EDX spectroscopy (**A**, **C**, **E**) and SEM (**B**, **D**, **F**). (A, B) Untreated discs (Ti6Al4V); (C, D) Ti-Ca-polyP discs fabricated with the lower concentration of APTMS (1 mg/assay; polyP@Ti6Al4V-l) in the polyP and $CaCl_2$ reaction assay; and (E, F) Ti-Ca-polyP discs which have been coated in the presence of higher APTMS concentration (2 mg/assay; polyP@Ti6Al4V-h).

Durability of the Ca-polyP coat

The surface coat of the polyP was measured by the determination of Ca^{2+} release from the coated discs in SBF (lacking Ca^{2+} as component), as described under "Materials and Methods". In parallel assays, the release of Ca^{2+} from Ti-Ca-polyP discs as well as from untreated titanium discs (control) was measured. As an additional control one Ti-Ca-polyP disc each was inserted in the SBF incubation medium supplemented with 1 µg/ml of ALP; all samples were incubated at 37°C.

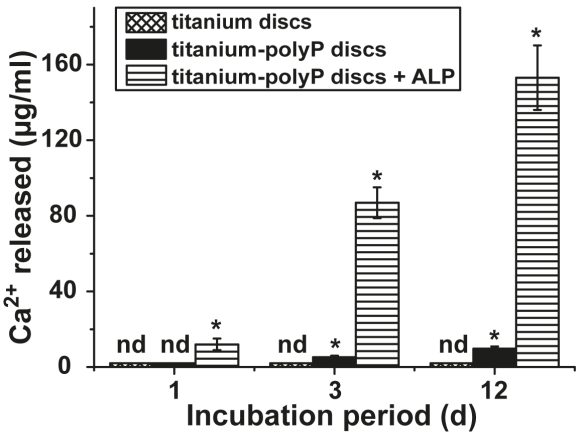

Fig. 5 Release of Ca^{2+} from untreated titanium discs (cross-striped bars), Ti-Ca-polyP discs (filled bars), as well as Ti-Ca-polyP discs, incubated together with alkaline phosphatase (ALP) (horizontally-striped bars). The discs had been incubated in assays (1 ml) with SBF as described under "Materials and Methods". "nd": the Ca^{2+} concentration in the assays had been non-determinable. Data are means ± SD of 5 independent experiments (***** $P < 0.01$).

The experiments revealed that at time zero in all three assays the Ca^{2+} concentration was < 3 µg/ml (non-determinable). After one d in the incubation medium the amount of Ca^{2+} concentration in assays containing Ti-Ca-polyP discs was still < 3 µg/ml, while in the samples with Ti-Ca-polyP discs + ALP the concentration of Ca^{2+} increased to 12 µg/ml (Fig. 5). The Ca^{2+} release increased slightly to 5 µg/ml in assays containing the Ti-Ca-polyP discs after a 3 d incubation period, in contrast to the assays of Ti-Ca-polyP discs together with ALP (87 µg/ml). After 12 d in the incubation assay the Ca^{2+} concentration in the samples with Ti-Ca-polyP discs amounted to 10 µg/ml, while in those containing Ti-Ca-polyP discs together with ALP the concentration was measured with 153 µg/ml (Fig. 5).

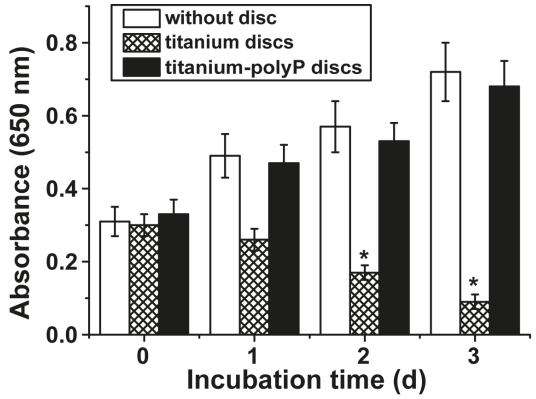

Fig. 6 Effect of titanium discs on growth of SaOS-2 cells. The cells were seeded, under otherwise identical conditions, into 24-well plates that did not contain titanium discs (open bars), titanium alloy discs (cross-striped bars) or Ti-Ca-polyP discs (filled bars). After an incubation period of 1, 2 and 3 d the cells were harvested and the viability of the cells was determined by the XTT assay. Data represent means ± SD of ten independent experiments (***** $P < 0.01$).

Growth of SaOS-2 cells on the titanium discs

The overall growth rate of the bone-like SaOS-2 cells was determined by the XTT assay as described under "Materials and Methods". The cells were seeded at a density of 3×10^4 cells/well (2 ml assays) for all three parallel series of experiments; assays without titanium discs, titanium alloy discs, Ti-Ca-polyP discs (Fig. 6). Already after a 1-d incubation period the density of the cells increased from 0.3 absorbance units to 0.49±0.6 units (assays without discs) and 0.47±0.05 units (with Ti-Ca-polyP discs), while the density in the assays with titanium alloy discs decreased to 0.26±0.03 units. This tendency increased during the following incubation days and reached values after 3-d incubation period of 0.09±0.02 (titanium alloy discs; significant reduction), 0.72±0.08 (absence of disc) and 0.68±0.07 (Ti-Ca-polyP discs). These data imply that the titanium surfaces are not supporting growth of the SaOS-2 cells, while the cells, growing on Ti-Ca-polyP discs showed the same growth kinetics like that of cultures without any discs.

The property of the discs, coated with polyP, being a very suitable matrix for SaOS-2 cells to grow onto, was also underscored by staining the surface of the discs. Titanium alloy discs, not coated with polyP (Fig. 7A) were incubated for 3 d with SaOS-2 cells; after that period no cells could be visualized onto the discs (Fig. 7C). In contrast, if polyP-coated Ti-Ca-polyP discs (Fig. 7B) are incubated in the presence of SaOS-2 cells for the same period of time an almost homogenous mono-cell layer is observed (Fig. 7D). A closer inspection at higher magnification revealed that the cells show the property of cell spreading (Fig. 7E and F), a characteristic sign for vital survival and growth of cells.[31]

As a further support of the conclusion that SaOS-2 cells are growing readily onto Ti-Ca-polyP discs the areas, covered with cells, were analyzed for the distribution of elements carbon (C) (Fig. 8B), titanium (Ti) (Fig. 8C) and phosphorus (P) (Fig. 8D). The semiquantitative determinations of the elements were performed by SEM-based EDX mappings. The localization of the cells was obtained by recording the back-scattered electrons (Fig. 8A). It is very much apparent that within the regions where the cells grow a high accumulation for the element C is measured (Fig. 8B), while titanium and polyP are highlighted outside of the cell areas, at the surrounding surface of the discs onto which the cells grow (Fig. 8C and D)

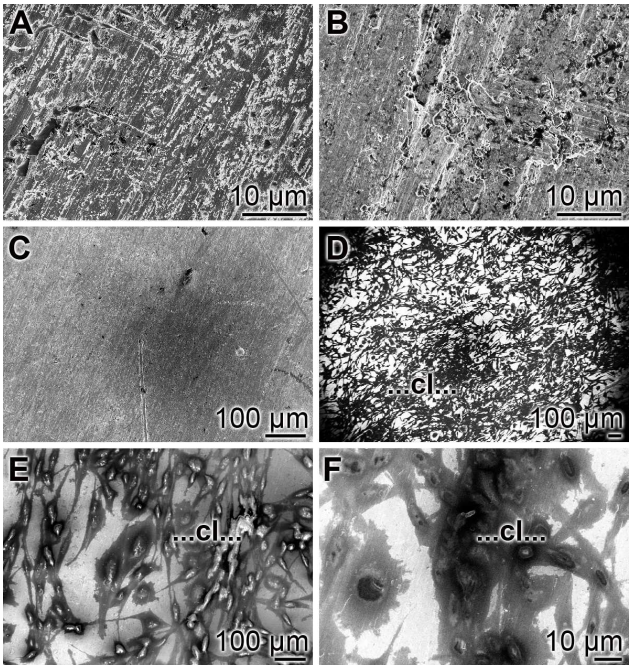

Fig. 7 Growth of SaOS-2 cells onto discs; SEM analysis. The cells were seeded into 24-well plates, containing either titanium alloy discs (**A**, **C**) or Ti-Ca-polyP discs (**B**, **D**-**F**). (A, B) Disc surfaces, prior to incubation with cells. (C) Surface of a titanium alloy disc after the 3 d incubation with SaOS-2 cells; no cells can be visualized. (D-F) In contrast, if the discs, covered with polyP, the Ti-Ca-polyP discs are inspected after a 3 d-incubation with the cells, a dense single-cell layer (cl) can be detected. (E and F) At a higher magnification the cells show the phenomenon of spreading.

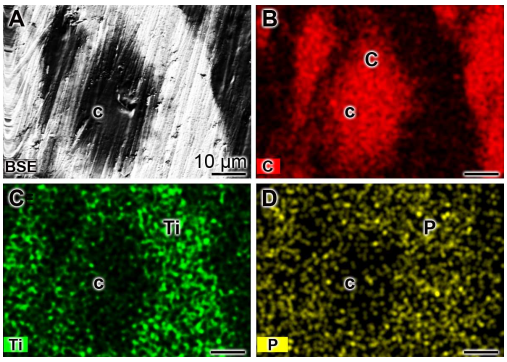

Fig. 8 Semiquantitative determinations of the elements carbon (C) (**B**), titanium (Ti) (**C**) and phosphorus (P) (**D**) along some cells, growing onto Ti-Ca-polyP discs after a 3 d incubation period. The cells (c) have been identified by back-scattered electrons (BSE). The element mapping was performed by SEM-based EDX scannings. The intensity of the respective pseudocolor signals for carbon (C), titanium (Ti) and phosphorous (P) correlate with the intensity of the generated X-rays. The cells were growing onto the disc for 3 d.

Expression of carbonic anhydrase IX and alkaline phosphatase

As a marker for the functional activity of the SaOS-2 cells, growing onto titanium discs, the expression of the two genes encoding for the enzymes carbonic anhydrase IX (CA IX) and alkaline phosphatase (ALP) was determined by quantitative qRT-PCR. The studies for the steady-state level of transcripts of CA IX in SaOS-2 cells growing for 3 d in the absence of the MAC showed for the cultures which contained titanium alloy discs a significant decrease of the expression levels from 0.31±0.03 (time at seeding) to 0.12±0.01, while the levels in the cells cultured in the absence of discs or the presence of the Ti-Ca-polyP discs increased from 0.27±0.02 and 0.25±0.03 to 0.38±0.04 and 0.40±0.05, respectively (Fig. 9A). We interpret the reduction of the expression of *CA IX* (day3) as a sign for the dieback and/or the reduced metabolism of the cells. A subsequent incubation of the cultures in the presence of the MAC resulted in an increase of the levels for the CA IX expression in assays that contained no discs or into which Ti-Ca-polyP discs have been submersed. After 5 d in the presence of the MAC a significant increase of the *CA IX* transcript level in cells in the absence of discs from 0.38±0.04 to 0.81±0.08 was detected. A pronounced increase of this gene was also found in cells, cultured onto Ti-Ca-polyP discs with 0.41±0.05 to 0.59±0.06. In contrast, no expression of *CA IX* is measured in assays with Ti-Ca-polyP discs, even after 3d. This finding might reflect that SaOS-2 cells die off faster if exposed to MAC, which activates cells metabolism in general.

In parallel, the expression of the gene for the enzyme ALP was determined, likewise by qRT-PCR. Again the data (Fig. 9B) show that the expression level of ALP in culture containing the titanium alloy discs significantly decrease after a 3 d incubation period the absence of any discs. Later during the incubation the level is so low, that the expression cannot documented reliably. In contrast, in the presence of the MAC the steady-state expression of the ALP increases significantly, both in the assays without discs and in the assays with Ti-Ca-polyP discs; from 0.038±0.005 to 0.097±0.7 (at day 5 without discs) and from 0.034±0.004 to 0.074±0.007, respectively.

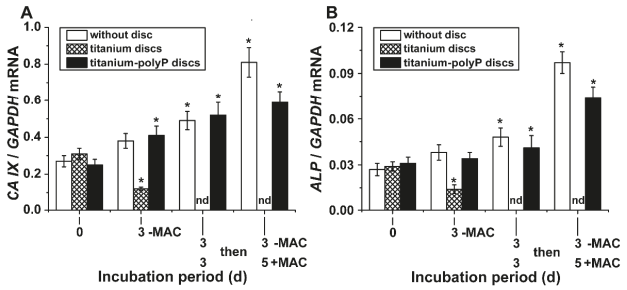

Fig. 9 Expression of the genes encoding for (**A**) CA IX and for (**B**) ALP. The expression values were normalized to the expression of *GAPDH*. The cells were cultivated either without any titanium discs (open bars), or either onto titanium alloy discs (cross-striped bars) or on Ti-Ca-polyP discs (filled bars). The cultures were incubated at first in the absence of the MAC for 3 d (-MAC); then they were transferred to medium, supplemented with the MAC (+MAC), and the incubation was continue for additional 3 or 5 d, as outlined. Then the cells were harvested, RNA was extracted and subjected to qRT-PCR for determination of both *CA IX* and *ALP* transcripts; the expression of *GAPDH* served as reference. Data are expressed as mean values ± SD for five independent experiments; each

experiment was carried out in duplicate (* $P < 0.01$ [the values at time zero were used as reference points]). nd, not detectable.

Morphology of the HA crystallites

SEM analyses were performed with SaOS-2 cells grown onto Ti-Ca-polyP discs for 5 d or 8 d in medium, containing MAC. While after 5 d no mineral nodules are seen onto SaOS-2 cells (Fig. 10A), distinct nodules had been formed onto cells after an incubation period of 8 d (Fig. 10B).

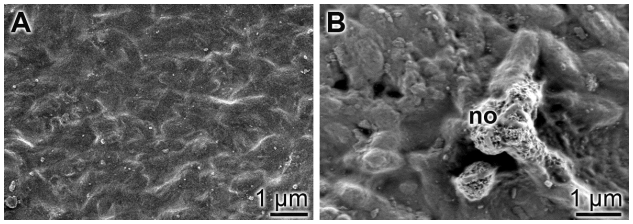

Fig. 10 Surface structure of SaOS-2 cells. The cultures were pre-incubated in the absence of MAC for 3 d; then they were transferred to medium, supplemented with the MAC, and the incubation was continue for additional 3 d (**A**) or 5 d (**B**). SEM images. As seen, mineral deposits/nodules (no) are formed onto SaOS-2 cells after an incubation period of 8 d in the presence of MAC (B).

Discussion

In the present study we succeeded to develop a procedure through which titanium/titanium alloy can be tightly overlaid with polyP. After etching with HCl the metal surface is covalently linked with APTMS, after which the Ca-polyP particles can attach to the surface via Ca^{2+} ionic linkages (scheme in Fig. 1). The polyP coat at the surface of the metal, on the Ti-Ca-polyP-discs, is considerable durable in SBF. If referred to the assays which did not contain additionally to the Ti-Ca-polyP discs the polyP-degrading enzyme ALP[8] [Ti-Ca-polyP discs], the release of calcium ions from the coated Ti-Ca-polyP discs was not detectable, while in the assay with the Ti-Ca-polyP discs + ALP the Ca^{2+} release in the medium amounted to 12±3 µg/ml (incubation period, 1 d). After a 3 d incubation period the release of Ca^{2+} increased in the assays with the Ti-Ca-polyP discs to 6% with respect to the Ti-Ca-polyP discs + ALP. After the 12 d incubation still only 6% of Ca^{2+} is released from the Ti-Ca-polyP discs. From this result we draw the conclusion that the Ca-polyP coat around the discs is surprisingly stable. Surely APTMS can be replaced by other silane coupling agents, e.g. 3-(trimethoxysilyl)propyl methacrylate;[30] however APTMS has a further functional group allowing – in addition to polyP – peptides to be bound to the silane-coated titanium surfaces.

EDX analyses revealed that on untreated titanium discs the elements phosphorus and calcium are almost totally absent. However, if the discs are coated with APTMS and additionally with Ca^{2+} and polyP these peaks become prominent. At the lower APTMS concentration, used for cross-linking the Ca-polyP microparticles can be resolved by SEM, while a continuous layer of Ca-polyP is seen if the higher APTMS concentration is present during the reaction. This result implies that the APTMS functionalized groups are more abundant, allowing a larger amount of polyP groups to react.

In contrast to the considerably high surface roughness of the untreated titanium discs with approximately 7 µm in maximum, Ti-Ca-polyP discs are smooth with a maximal roughness of 0.8 µm. Usually the degree of cell attachment to very smooth surfaces is lower, compared to moderately rougher surfaces (e.g. ref.[32]). Therefore, it came unexpected that the polyP-coated discs allow SaOS-2 cells to grow with a rate, seen in control assays without any discs. Indicative is the finding that the cells in the assays, which contained untreated titanium discs die off after an incubation period of 2 d. Microscopic inspection supported this assumption. After incubation for 3 d no cells could be visualized onto the discs. This is very much in contrast to the observation that during the same period of time SaOS-2 cells densely attach to the Ti-Ca-polyP discs and form an almost homogenous mono-cell layer. Amazing is the finding that the cells growing on the Ti-Ca-polyP discs show the phenotypic morphology of cell spreading. Cell-spreading behavior is a clear sign for an active cell metabolism and cell migration.[33] In the present study we used titanium oxidized Ti-6Al-4V discs that showed adverse properties for cells to grow onto. In contrast, in earlier studies and using pure titanium disks, it had been reported that those surfaces allow cells to attach and to grow. [34,35]

In order to prove that the cells, growing on Ti-Ca-polyP discs show distinct functional gene expression the steady-state levels of transcripts encoding for the CA IX, as well as for the ALP have been quantified by qRT-PCR (reviewed in: ref.[36]). The enzyme CA IX is the main CA that is cell membrane-bound and most likely primarily involved in the initiation of bone formation. Considerable experimental evidence is available that during the initial phase of bone mineral formation $CaCO_3$ deposits are formed.[36] This process is enzymatically driven by the enzyme CA.[37] Recently, our group obtained experimental evidence that it is the CA IX which is mainly involved in this process (Müller et al. submitted). The ALP is one of the most established markers for functionally active, mineral deposit forming osteoblasts (see: ref.[38]). The expression studies, summarized here, impressively show that the transcript steady-state levels of both genes, *CA IX* and *ALP*, significantly increase in SaOS-2 cells to an extent that is measured also in cells growing in the absence of discs. Interesting is also the fact that the transcript levels of these two genes, *CA IX* and *ALP*, significantly drop during the incubation onto untreated titanium discs.

Since the polyP layer onto the titanium discs will be enzymatically hydrolyzed by the ALP it is assumed that during this period the tissue cells will be attracted by the polymer and will change the surface of the metal with a "biological" coat, e.g. fibronectin, laminin and subsequently with collagen, allowing a tight interaction between the cells and the metal implant.

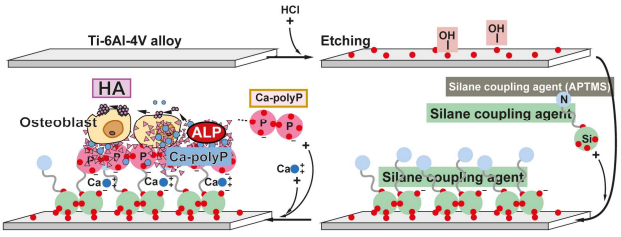

Fig. 11 Coating of titanium discs with morphogenetically active Ca-polyP. The metal material (Ti-6Al-4V) acquires bio-functional properties if coated with the morphogenetically active Ca-polyP polymer. During the process the titanium surfaces becomes etched, resulting in the exposure of hydroxyl groups. At a pH of 8 they form covalently linkages with siliane coupling agents, e.g. APTMS. Under this environment Ca^{2+}-ionic bridges are formed between the silane and polyP. Those coated titanium discs allow bone-like SaOS-2 cells to settle on and induce them to gene expression (*CA IX* and *ALP*); these enzymes are crucially involved in bone-mineral/hydroxyapatite (HA) deposition.

Conclusions

Taking together, the data gathered here show that titanium discs, titanium oxidized Ti-6Al-4V scaffolds, are inert matrices for bone-like SaOS-2 cells *in vitro*. This metal material acquires bio-functional properties if coated with the morphogenetically active Ca-polyP polymer (Fig. 11). Titanium alloy as used here in form of discs is used for the fabrication of implants.[39] The progress in the biological functionalization of this (potential) implant material with polyP offers not only the fabrication of individualized implants but also provides the advantageous property to match the mechanical properties of the hard and brittle metal implant with those of the softer bone and its surrounding tissue.

Acknowledgements

W.E.G. M. is a holder of an ERC Advanced Investigator Grant (No. 268476 BIOSILICA). We thank Ms. Maren Müller ("Elektronenmikroskopie"; Max Planck Institute for Polymer Research, Mainz, Germany) for very expert and helpful EDX analyses. This work was supported by grants from the European Commission (ERC Advanced Investigator Grant "BIOSILICA": No. 268476; "Bio-Scaffolds": No. 604036 and "BlueGenics": No. 311848), the Deutsche Forschungsgemeinschaft (Schr 277/10-3), and the International Human Frontier Science Program.

References

1 U. Meyer, The history of tissue engineering and regenerative medicine in perspective, in: U. Meyer, T. Meyer, J. Handschel and H.P. Wiesmann (Eds.), Fundamentals of Tissue Engineering and Regenerative Medicine, Springer Press, Berlin-Heidelberg, 2009, pp. 5-12.
2 M. Epple, Biomimetic bone substitution materials, in: M. Epple and E. Baeuerlein (Eds.), Biomineralisation: Medical and Clinical Aspects, Wiley-VCH, Weinheim, Germany, 2007, pp. 81–95.
3 S.S. Jensen and H. Terheyden, Bone augmentation procedures in localized defects in the alveolar ridge: clinical results with different bone grafts and bone-substitute materials, Int. J. Oral Maxillofac. Implants, 2009, **24 Suppl**, 218-236.
4 I.V. Yannas, Emerging rules for inducing organ regeneration, Biomaterials, 2013, **34**, 321-330.
5 U. Schloßmacher, H.C. Schröder, X.H. Wang, Q. Feng, B. Diehl-Seifert, S. Neumann, A. Trautwein and W.E.G. Müller, Alginate/silica composite hydrogel as a potential morphogenetically active scaffold for three-dimensional tissue engineering, RSC Advances, 2013, **3**, 11185–11194.
6 X.H. Wang, H.C. Schröder and W.E.G. Müller, Enzymatically synthesized inorganic polymers as morphogenetically active bone scaffolds: application in regenerative medicine, Int. Rev. Cell Mol. Biol., 2014, **313**, 27-77.
7 W.E.G. Müller, E. Tolba, H.C. Schröder and X.H. Wang, Polyphosphate: a morphogenetically active implant material serving as metabolic fuel for bone regeneration, Macromolec. Biosci., 2015, doi: 10.1002/mabi.201500100.
8 W.E.G. Müller, E. Tolba, H.C. Schröder, S, Wang, G. Glaßer, R. Muñoz-Espí, T. Link and X.H. Wang, A new polyphosphate calcium material with morphogenetic activity, Materials Letters, 2015, **148**, 163-166.
9 W.E.G. Müller, E. Tolba, H.C. Schröder, B. Diehl-Seifert and X.H. Wang, Retinol encapsulated into amorphous Ca^{2+} polyphosphate nanospheres acts synergistically in MC3T3-E1 cells, Eur. J. Pharm. Biopharm., 2015, **93**, 214-223.
10 W.E.G. Müller, E. Tolba, Q. Feng, H.C. Schröder, J.S. Markl, M. Kokkinopoulou and X.H. Wang, Amorphous Ca2+ polyphosphate nanoparticles regulate the ATP level in bone-like SaOS-2 cells, J. Cell Sci., 2015, **128**, 2202-2207.
11 J.P. Li, J.R. de Wijn, C.A. Van Blitterswijk and K. de Groot, Porous Ti6Al4V scaffold directly fabricating by rapid prototyping: preparation and *in vitro* experiment, Biomaterials, 2006, **27**, 1223-1235.
12 A.L. Jardini, M.A. Larosa, L.F. Bernardes, C.A.C. Zavaglia and R. Maciel-Filho, Application of direct metal laser sintering in titanium alloy for cranioplasty, 6º Congr Brasiliero de Engenharia de Fabrica, Caxias do Sul, Brasil, 11.-15.4.2011.
13 G. Han, W.E.G. Müller, X.H. Wang, L. Lilja and Z. Shen, Porous titania surfaces on titanium with hierarchical macro- and mesoporosities for enhancing cell adhesion, proliferation and mineralization, Mater. Sci. Eng. C Mater. Biol. Appl., 2015, **47**, 376-383.
14 C. Wang, H. Mao, C. Wang and S. Fu, Dispersibility and hydrophobicity analysis of titanium dioxide nanoparticles grafted with silane coupling agent, Ind. Eng. Chem. Res., 2011, **50**, 11930-11934.
15 S.B. Rodan, Y. Imai, M.A. Thiede, G. Wesolowski, D. Thompson, Z. Bar-Shavit, S. Shull, K. Mann and G.A. Rodan, Characterization of a human osteosarcoma cell line (Saos-2) with osteoblastic properties, Cancer Res., 1987, **47**, 4961-4966.
16 S.T. Meikle, G. Bianchi, G. Olivier and M. Santin, Osteoconductive phosphoserine-modified poly({varepsilon}-lysine) dendrons: synthesis, titanium oxide surface functionalization and response of osteoblast-like cell lines, J. R. Soc. Interface, 2013, **10**, 20120765, doi: 10.1098/rsif.2012.0765.
17 S.H. Ye, C.A. Johnson Jr, J.R. Woolley, H.I. Oh, L.J. Gamble, K. Ishihara and W.R. Wagner, Surface modification of a titanium alloy with a phospholipid polymer prepared by a plasma-induced grafting technique to improve surface thromboresistance, Colloids Surf. B Biointerfaces, 2009, **74**, 96-102.
18 S.H. Ye, C.A. Johnson Jr, J.R. Woolley, T.A. Snyder, L.J. Gamble and W.R. Wagner, Covalent surface modification of a titanium alloy with a phosphorylcholine-containing copolymer for reduced thrombogenicity in cardiovascular devices, J. Biomed. Mater. Res. A, 2009, **91**, 18-28.
19 T. Kokubo, H. Kushitani, S. Sakka, T. Kitsugi and T. Yamamuro, Solutions able to reproduce *in vivo* surface-structure changes in bioactive glass-ceramic A-W, J. Biomed. Mater. Res., 1990, **24**, 721-734.
20 F.H. Pollard and J.V. Martin, The spectrophotometric determination of the alkaline-earth metals with murexide, eriochrome black T and with o-cresolphthalein complexone, Analyst, 1956, **81**, 348-353.

21 W.E.G. Müller, X.H. Wang, B. Diehl-Seifert, K. Kropf, U. Schloßmacher, I. Lieberwirth, G. Glasser, M. Wiens and H.C. Schröder, Inorganic polymeric phosphate/polyphosphate as an inducer of alkaline phosphatase and a modulator of intracellular Ca^{2+} level in *osteoblasts (*SaOS-2 cells) *in vitro*. Acta Biomaterialia, 2011, **7**, 2661-2671.
22 T. Salge and R. Terborg, EDS microanalysis with the silicon drift detector (CDD): innovative analysis options for mineralogical and material science application, Anadolu Univ. J. Sci. Technol., 2009, **10**, 45–55.
23 M. Wiens, X.H. Wang, U. Schlossmacher, I. Lieberwirth, G. Glasser, H. Ushijima, H.C. Schröder and W.E.G. Müller, Osteogenic potential of biosilica on human osteoblast-like (SaOS-2) cells, Calcif. Tissue Int., 2010, **87**, 513-524.
24 K. Mori, M. Berreur, F. Blanchard, C. Chevalier, I. Guisle-Marsollier, M. Masson, F. Rédini and D. Heymann, Receptor activator of nuclear factor-kappaB ligand (RANKL) directly modulates the gene expression profile of RANK-positive Saos-2 human osteosarcoma cells, Oncol. Rep., 2007, **18**, 1365–1371.
25 T. Hondo, T. Kanaya, I. Takakura, H. Watanabe, Y. Takahashi, Y. Nagasawa, S. Terada, S. Ohwada, K. Watanabe, H. Kitazawa, M.T. Rose, T. Yamaguchi and H. Aso, Cytokeratin 18 is a specific marker of bovine intestinal M cell, Am. J. Physiol. Gastrointest. Liver Physiol., 2011, **300**, G442-G453.
26 M. Wiens, X.H. Wang, H.C. Schröder, U. Kolb, U. Schloßmacher, H. Ushijima and W.E.G. Müller, The role of biosilica in the osteoprotegerin/RANKL ratio in human osteoblastlike cells, Biomaterials, 2010, **31**, 7716-7725.
27 W.E.G. Müller, X.H. Wang, V. Grebenjuk, B. Diehl-Seifert, R. Steffen, U. Schloßmacher, A. Trautwein, S. Neumann and H.C. Schröder, Silica as a morphogenetically active inorganic polymer: effect on the BMP-2-dependent and RUNX2-independent pathway in osteoblast-like SaOS-2 cells, Biomaterials Sci., 2013, **1**, 669-678.
28 M.W. Pfaffl, A new mathematical model for relative quantification in real-time RT-PCR, Nucleic Acids Res., 2001, **29**, 2002–2007.
29 L. Sachs, Angewandte Statistik, Springer, Berlin, 1984, p. 242.
30 G. Chen and J.S. Yoon, Nanocomposites of poly[(butylenes succinate)-*co*-(butylene adipate)] (PBSA) and twice-functionalized organoclay, Polym. Int., 2005, **54**, 939-945.
31 L.S. Price, Morphological control of cell growth and viability, Bioessays, 1997, **19**, 941-943.
32 H.H. Huang, C.T. Ho, T.H. Lee, T.L. Lee, K.K. Liao and F.L. Chen, Effect of surface roughness of ground titanium on initial cell adhesion, Biomol. Eng., 2004, **21**, 93-97.
33 B. Huang, M. Lu, M.K. Jolly, I. Tsarfaty, J. Onuchic and E. Ben-Jacob, The three-way switch operation of Rac1/RhoA GTPase-based circuit controlling amoeboid-hybrid-mesenchymal transition, Sci. Rep., 2014, **4**, 6449; doi: 10.1038/srep06449.
34 I. Degasne, M.F. Baslé, V. Demais, G. Huré, M. Lesourd, B. Grolleau, L. Mercier and D. Chappard, Effects of roughness, fibronectin and vitronectin on attachment, spreading, and proliferation of human osteoblast-like cells (Saos-2) on titanium surfaces, Calcif. Tissue Int., 1999, **64**, 499-507.
35 L. Postiglione, G. Di Domenico, L. Ramaglia, S. Montagnani, S. Salzano, F. Di Meglio, L. Sbordone, M. Vitale and G.Rossi, Behavior of SaOS-2 cells cultured on different titanium surfaces, J. Dent. Res., 2003, **82**, 692-696.
36 X.H. Wang, H.C. Schröder and W.E.G. Müller, Enzyme-based biosilica and biocalcite: biomaterials for the future in regenerative medicine, Trends Biotechnol., 2014, **32**, 441-447.
37 W.E.G. Müller, H.C. Schröder, U. Schlossmacher, V.A. Grebenjuk, H. Ushijima and X.H. Wang, Induction of carbonic anhydrase in SaOS-2 cells, exposed to bicarbonate and consequences for calcium phosphate crystal formation, Biomaterials, 2013, **34**, 8671-8680.
38 X.H. Wang, H.C. Schröder, M. Wiens, H. Ushijima and W.E.G. Müller, Bio-silica and bio-polyphosphate: applications in biomedicine (bone formation), Current Opinion Biotechnol., 2012, **23**, 570–578.
39 J.P. Li, J.R. de Wijn, C.A. van Blitterswijk and K. de Groot, The effect of scaffold architecture on properties of direct 3D fiber deposition of porous Ti6Al4V for orthopedic implants, J. Biomed. Mater. Res. A, 2010, **92**, 33-42.

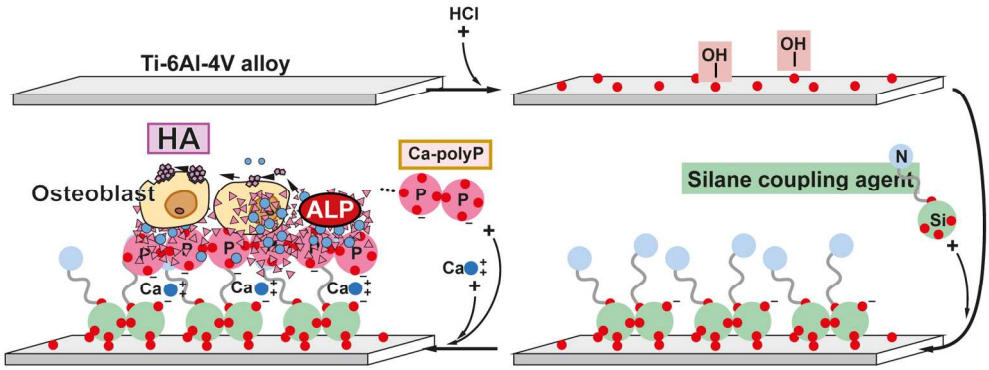

161x61mm (300 x 300 DPI)